

Mechanisms for the formation of epoxide and chlorine-containing products in the oxidation of ethylene by chromyl chloride: a density functional study

Maricel Torrent, Liqun Deng, Miquel Duran, Miquel Solà, and Tom Ziegler

Abstract: The reaction between CrO_2Cl_2 and ethylene leading to the formation of epoxide and chlorohydrin precursors or directly to 1,2-dichloroethane has been studied by density functional theory. The formation of the epoxide precursor ($\text{Cl}_2(\text{O})\text{Cr}-\text{OC}_2\text{H}_4$) was found to take place via a [3+2] addition of ethylene to two Cr=O bonds followed by rearrangement of the five-membered diol to the epoxide product. The alternative mechanisms involving a direct addition of oxygen to ethylene or the [2+2] addition of the olefin to a Cr=O bond were found to have much higher activation energies. The formation of the chlorohydrin precursor ($\text{Cl}(\text{O})\text{Cr}-\text{OCH}_2=\text{CHCl}$) was found to take place via a [3+2] addition to one Cr—Cl and one Cr=O bond. Pathways involving initial [2+2] addition to a Cr—Cl or Cr=O bond had much higher activation barriers. The generation of 1,2-dichloroethane is highly unfavorable with an endothermicity of 44.7 kcal/mol and an even higher activation barrier. It is suggested that the formation of epoxide and chlorohydrin from the respective precursors requires the addition of H_2O .

Key words: reaction mechanisms, epoxide, oxidation of ethylene, chromyl chloride, DFT.

Résumé : Faisant appel à la théorie de la densité fonctionnelle, on a étudié la réaction du CrO_2Cl_2 avec l'éthylène qui conduit à la formation de précurseurs époxyde et chlorohydrine ou directement de 1,2-dichloroéthane. On a trouvé que la formation du précurseur époxyde [$\text{Cl}_2(\text{O})\text{Cr}-\text{OC}_2\text{H}_4$] se produit par le biais d'une addition [3+2] de l'éthylène sur deux liaisons Cr=O, suivie d'un réarrangement du diol à cinq chaînons en produit époxyde. On a trouvé que les autres mécanismes possibles, addition directe d'oxygène à l'éthylène ou l'addition [2+2] de l'oléfine sur une liaison Cr=O, comportent des énergies d'activation beaucoup plus élevées. On a trouvé que la formation du précurseur chlorohydrine [$\text{Cl}(\text{O})\text{Cr}-\text{OCH}_2=\text{CHCl}$] se fait par le biais d'une addition [3+2] sur une liaison Cr—Cl et une sur une liaison Cr=O. Les voies réactionnelles impliquant une addition [2+2] initiale à une liaison Cr—Cl ou Cr=O comportent des barrières d'activation beaucoup plus élevées. La formation de 1,2-dichloroéthane est très défavorisée par son grand caractère endothermique (44,7 kcal/mol) et sa barrière d'activation encore plus élevée. Il est suggéré qu'une addition d'eau est nécessaire pour la formation de l'époxyde et de la chlorohydrine à partir de leurs précurseurs respectifs.

Mots clés : mécanismes réactionnels, époxyde, oxydation de l'éthylène, chlorure de chromyle, « DFT ».

[Traduit par la Rédaction]

I. Introduction

The oxygen-transfer reaction from CrO_2Cl_2 to olefins is an old (1) and now well-established process (2). Unlike other oxo transition metal compounds, CrO_2Cl_2 reacts with alkenes to form predominantly an epoxide product, whereas KMnO_4 and OsO_4 form diols without significant epoxide formation (3). Some time ago it was found that, in fact, the three primary products in the oxidation of alkenes with CrO_2Cl_2 are epoxide, chlorohydrin, and, in some cases, vicinal dichloride (4, 5). The full mechanism by which these

products are formed still remains unsolved despite having been the subject of extensive studies (6–9).

To explain the formation of the abovementioned products, Sharpless et al. (5) originally proposed a mechanism involving organometallic intermediates with Cr—C σ bonds. In particular, the key feature in the formation of epoxide was claimed to be the involvement of a chromaoxetane, i.e., a four-membered cyclic compound formed via a [2+2] interaction between the olefin and an oxo group on the chromium (5). This mechanism was very much contrary to the previously suggested mechanisms for this reaction in which a di-

Received December 15, 1998.

M. Torrent, M. Duran, and M. Solà. Department of Chemistry, and Institute of Computational Chemistry, University of Girona, Girona E-17071, Catalonia, Spain.

L. Deng and T. Ziegler.¹ Department of Chemistry, University of Calgary, Calgary, AB T2N 1N4, Canada.

¹Author to whom correspondence may be addressed. Telephone: (403) 220-5368. Fax: (403) 289-9488.
e-mail: ziegler@zinc.chem.ucalgary.ca

rect interaction between the alkene and the oxo groups of CrO_2Cl_2 had been postulated (1, 6).

Although the new idea was suggested as an alternative path based only on the observed products of the reaction (no evidence for a chromaoxetane intermediate was established), it was quickly adapted within a few years in the discussion of many types of oxygen-transfer reactions involving high-valent oxochromium compounds (10) and other oxo-transition metal species (11). The advantage of the novel proposal was that experimental observations concerning *cis* addition (5) could now be more easily accommodated. Sharpless et al. (5), however, introduced their hypothesis with reserve because some mechanisms involving direct interaction with the ligands were able to account for experimental facts as well. Particularly, neither a direct addition of the olefin to one oxygen atom nor a [3+2] addition of the olefin to two heteroatom ligands could be excluded at that time as operative routes for the mechanism of epoxidation. Some years later, Samsel et al. (7) argued for a direct interaction between the alkene and the oxygen in OCr(V) -salen complexes in the epoxidation of alkenes, rather than a chromaoxetane. Some interesting results that cast doubt on the metallaoxetane reaction path were also reported by Barrett et al. (12), and later on by Groves and Nemo (13). To date, experimental input has not been sufficient to rule out either of the mechanistic channels.

To obtain further insight into the sequence of this reaction, some theoretical contributions have appeared. The most notable earlier computational study is that of Rappé et al. (8, 9) where a thermodynamic analysis by means of the generalized valence bond method was performed, with attention being devoted to the energies of the intermediates in the oxidation of ethylene with CrO_2Cl_2 and MoO_2Cl_2 . Unfortunately, due to limitations in methodology and computational facilities at that time, these authors were not able to fully optimize the geometrical structures of the different species involved. Their results favored a [2+2] cycloaddition path involving a four-centered intermediate, and confirmed the proposal that the metallaoxetane is a likely common precursor for all of the observed oxygen-containing products (8).

Further theoretical support for a chromaoxetane was provided (14) later by an *ab initio* study of the addition of ethylene to $\text{Cr}=\text{O}^{n+}$ ($n = 1-3$). Several gas-phase investigations have also supported the chromaoxetane as an intermediate in the reaction of oxochromium species with alkenes (15). In fact, the metallaoxetane intermediate derived from a [2+2] cycloaddition has been proposed in many other studies of oxygen-transfer reactions from oxomanganese and oxoiron porphyrins to alkenes (11), but often without detailed mechanistic investigations or without any direct experimental evidence to support it (16). A few isolated metallaoxetanes are known for Rh (17), Ir (18), Pd (19), and Pt (20). However, none of these species were synthesized by direct addition of olefin to a $\text{M}=\text{O}$ bond. Also to date no chromaoxetane has been isolated.

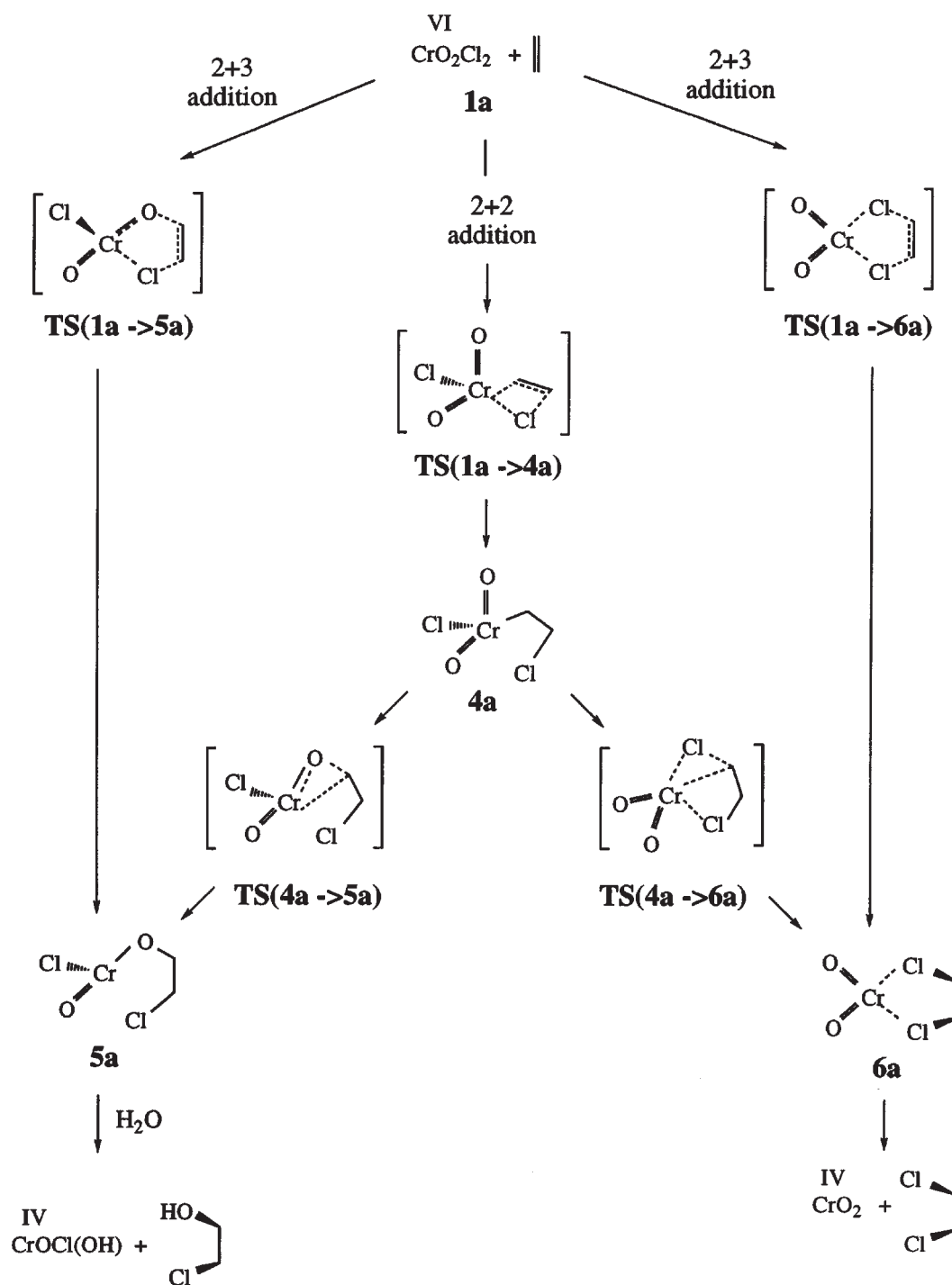
It appears that at least three different reaction modes have been used to explain the formation of epoxide (Scheme 1): (1) a direct addition of ethylene to one oxygen atom, (2) a [2+2] addition of ethylene to one $\text{Cr}=\text{O}$ linkage, and (3) a [3+2] addition to two $\text{Cr}=\text{O}$ bonds. However, what appears

to have been forgotten, at least in some of the proposed mechanisms, is that the reaction $\text{CrCl}_2\text{O}_2 + \text{C}_2\text{H}_4 \rightarrow \text{CrCl}_2\text{O} + \text{C}_2\text{H}_4\text{O}$ is endothermic with an experimental heat of reaction (21) given by 24.8 kcal/mol. Thus, the intermediates formed in the three mechanisms will not spontaneously decompose to epoxide. In fact, experimentally, epoxide is only isolated after the original reaction mixture in an organic solvent (such as CH_2Cl_2) is extracted into aqueous solution. Thus, it is likely that epoxide is formed from the reaction of water with one or more of the precursors in Scheme 1. Regarding the formation of the chlorine-containing products (Scheme 2), both a [2+2] and (or) a [3+2] cycloaddition pathway can account in principle for the mechanisms leading to a chlorohydrin (left) precursor and dichloride (right). However, again for the chlorohydrin (left) precursor a hydrogen containing agent such as water is needed to release $\text{CH}_2(\text{OH})\text{CH}_2\text{Cl}$.

In the present paper, the pathways outlined in Schemes 1 and 2 are explored in terms of reaction energies and activation barriers. The objective of our study is (i) to examine the energetics and kinetics of the mechanism leading to the epoxide precursors of Scheme 1 when ethylene is oxidized by CrO_2Cl_2 , (ii) to provide an interpretation for the formation of chlorohydrin precursor of Scheme 2 as one of the main products in the reaction of CrO_2Cl_2 with ethylene, and (iii) to rationalize why only in some cases dichloride is observed among the products. Finally, we shall briefly discuss the thermochemistry of the reaction between H_2O and the precursors in Schemes 1 and 2. To the best of our knowledge, this is the first time that mechanistic insight is given into the formation of epoxide, chlorohydrin, and dichloride using optimization procedures, and transition state search schemes.

II. Computational details

The reported calculations were carried out using the Amsterdam Density Functional (ADF) package developed by Baerends et al. (22a), and vectorized by Ravenek (22b). The adopted numerical integration procedure was due to te Velde et al. (23). A set of auxiliary *s*, *p*, *d*, *f*, and *g* STO functions, centered on all nuclei, were introduced in order to fit the molecular density and Coulomb potential accurately in each SCF cycle (24). An uncontracted STO basis set was employed for the valence orbitals of the chromium atom (double- ζ 3*s* and 3*p*, triple- ζ 3*d* and 4*s*, and a single- ζ 4*p* orbital). For carbon (2*s*, 2*p*), oxygen (2*s*, 2*p*), chlorine (3*s*, 3*p*), and hydrogen (1*s*), use was made of a double- ζ basis set augmented by an extra polarization function (25). The fully occupied inner shells of chlorine and chromium (1*s*2*s*2*p*), as well as carbon and oxygen (1*s*) were assigned to the cores and treated by the frozen-core approximation (26). All the geometries and frequencies were calculated at the local density approximation (LDA) level (27) with the parametrization of Vosko et al. (28). The relative energies were evaluated by including Becke's nonlocal exchange (29) and Perdew's nonlocal correlation corrections (30) as perturbations based on the LDA density. This approach is denoted NL-P, and its validity to treat CrO_2X_2 (X = halogen) complexes (31) and similar systems (32) has been demonstrated elsewhere. The

Scheme 2. Mechanisms for the formation of chlorohydrin (left) and dichloride (right).

and co-workers (51) in a study that employed an extended basis set and the B3LYP functionals to calculate reaction enthalpies for oxidation of ethylene by a series of Re–oxo complexes. It can be deduced from Table 2 that the root mean square difference between Rappé estimates and our corresponding values is 1.8 kcal/mol with a maximum discrepancy of 2.9 kcal/mol. Again, this comparison indicates that the basis set we used can produce reliable relative energies for the systems under investigation.

III. Results and discussion

The first part of this section is dedicated to thoroughly analyze three different mechanistic proposals for the formation of epoxide precursor in terms of reaction energies and activation barriers. This is, in fact, the main goal of the present paper. The second part is devoted to the elucidation of the reaction steps leading to the formation of chlorohydrin precursor, together with the characterization of the main inter-

Table 1. Comparison of the DFT values with the experimental data for the reaction enthalpies of the oxidation of olefin.

Reaction ^a	Energy (kcal/mol)	
	BP86 ^b	Expt.
CrO ₂ Cl ₂ + C ₂ H ₄ → CrOCl ₂ + epoxide	26.7 (29.2 ^c)	24.8 ^d
CrO ₂ Cl ₂ + C ₂ H ₄ → CrOCl ₂ + acetaldehyde	1.7 (3.7 ^c)	-3 ^e
CrO ₂ F ₂ + C ₂ H ₄ → CrOF ₂ + epoxide	28.0	23.2 ^d
Cp*ReO ₃ + C ₂ H ₄ → Cp*ReO(OCH ₂ CH ₂ O)	-2.8	-5 ± 3 ^f
Cp*ReO ₃ + C ₂ H ₄ → Cp*ReO ₂ + epoxide	32.6	
Cp*ReO ₃ + norbornene → Cp*Re(O)(1,2-norbornanediolate)	-8.0	-10.9 ± 0.9 ^f
Cp*ReO ₃ + norbornene → Cp*ReO ₂ + norbornene epoxide	28.0	

^aCrOCl₂ and CrOF₂ have triplet ground state, all the rest species have singlet ground state.

^bUnless otherwise specified, all ADF calculations were carried out with double- ζ plus polarization basis set for nonmetals (the standard ADF basis set III), and triple- ζ for Cr and Re atoms (the standard ADF basis set IV).

^cADF calculations were performed with triple- ζ plus 3*d* and 4*f* polarization functions for C and Cl atoms, triple- ζ plus 2*p* and 3*d* polarization functions for H, and triple- ζ plus two 4*f* functions for Cr; the basis set for the nonmetals was taken from standard ADF basis set V, and the basis set IVB of ref. 49 was used for Cr atom.

^dReference 21*a*.

^eReference 21*b*.

^fReference 50.

Table 2. Comparison of calculated reaction enthalpies by the BP86 and B3LYP functionals for the reactions LReO₃ + C₂H₄ → LRe(OCH₂CH₂O)^a.

Reaction ^a	Energy (kcal/mol)	
	BP86 ^b	B3LYP ^c
Cp*ReO ₃ + C ₂ H ₄ → Cp*ReO(OCH ₂ CH ₂ O)	-2.8	-4
CpReO ₃ + C ₂ H ₄ → CpReO(OCH ₂ CH ₂ O)	-5.7	-8
ClReO ₃ + C ₂ H ₄ → ClReO(OCH ₂ CH ₂ O)	17.4	16
(OH)ReO ₃ + C ₂ H ₄ → (OH)ReO(OCH ₂ CH ₂ O)	19.5	19
(OCH ₃)ReO ₃ + C ₂ H ₄ → (OCH ₃ O)ReO(OCH ₂ CH ₂ O)	19.9	17
CH ₃ ReO ₃ + C ₂ H ₄ → CH ₃ ReO(OCH ₂ CH ₂ O)	30.6	31
(O)ReO ₃ ⁻ + C ₂ H ₄ → (O)ReO(OCH ₂ CH ₂ O) ⁻	30.9	33

^aThe BP86 calculations show that (i) all species have singlet ground state, and (ii) the singlet and triplet states of the diolate ClReO(OCH₂CH₂O) are nearly degenerated.

^bThis work, BP86 calculations were carried out with double- ζ plus polarization basis set (ADF standard basis set III/H, C.1*s*, O.1*s*, Cl.2*p*) for nonmetal atoms, and triple- ζ basis set (ADF standard basis set IV/Re.4*f*) for Re atom, geometries were optimized by the quasiself-consistent method (ref. 52).

^cReference 51, the B3LYP results were based on the geometries optimization with 6-31G* basis set for nonmetals, and the modified LANL2DZ basis with a single *f* function for Re, and the relative energies were determined by single-point calculations at the minima using an extended basis in which the metal *f* function was replaced by two, and the nonmetal basis set expanded to 6-31+G*.

mediates and TS structures involved in the potential energy surface (PES) of the two suggested paths. Finally, the formation of dichloride is also discussed.

III.1. Formation of the epoxide precursor

The CrO₂Cl₂-mediated transformation of ethylene to epoxide can be viewed as a one-oxygen atom transfer reaction. As seen from Scheme 1, it involves formally a reduction of the metal center from Cr(VI) *d*⁰ in the reactants, **1a**, to Cr(IV) *d*² in the products. Regardless of the path leading to epoxide, a common direct precursor in all suggested mechanisms has been species **1b** (Fig. 1). This species was already postulated by Sharpless et al. (5) as the immediate precursor of epoxide, and more recently (21*b*), also as the oxirane adduct intermediate leading to acetaldehyde. The two forming C—O bond distances are certainly close to the ones in the final epoxide (1.416 Å), and the C—C bond is no longer the double bond in ethylene (1.323 Å). We find that **1b** has a *d*² configuration with a triplet ground state. We

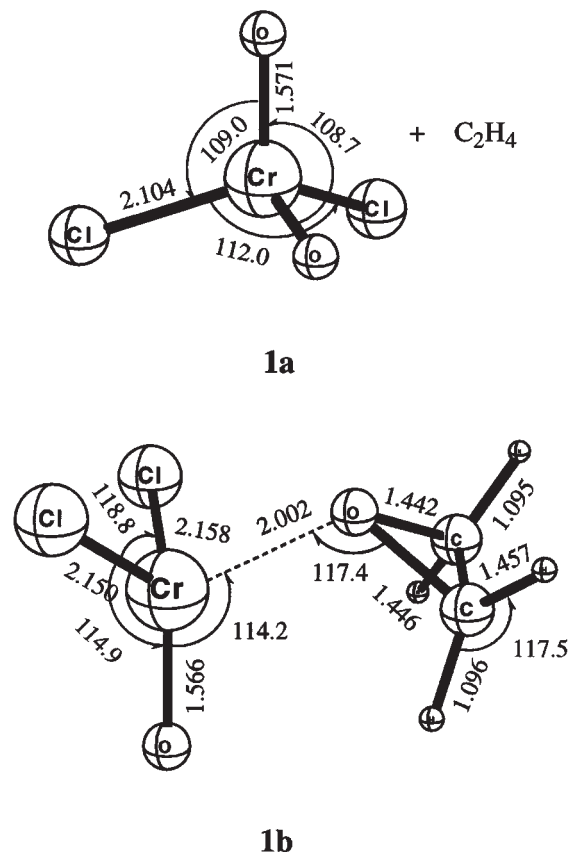
shall in the following discuss the energetics and kinetics for the suggested mechanisms leading to **1b**.

Figure 2 summarizes the energy profiles for the three mechanisms we are going to describe in the following paragraphs. Energetic aspects will be discussed in connection to the molecular structures obtained for each path (Figs. 3–6) following the sequence: direct addition, [2+2] cycloaddition, and [3+2] cycloaddition.

Starting from **1a**, the possible routes leading to **1b** can be classified according to the number of steps required in the transformation. Either the [2+2] or the [3+2] cycloaddition turns out to be two-step processes. A possible alternative to these routes is the apparently more simple direct addition of ethylene to one of the oxygen atoms in a single step. Since the ground-state structures of **1a** and **1b** lie on different PESs (singlet and triplet, respectively), a crossing point is expected to be found somewhere along the reaction path.

Figure 3 displays the optimized geometries of the two possible transition states connecting **1a** and **1b**:

Fig. 1. Optimized geometrical parameters of reactants **1a** and intermediate **1b**. Distances in Å, and angles in degrees.



TS(1a→1b)/s (*s* = singlet) and **TS(1a→1b)/t** (*t* = triplet). Geometrical analysis reveals that the former TS resembles species **1b** (elongation of the Cr—O bond and stretching of the C—C bond to similar extents) whereas, in the latter, both the olefin and the metal fragment mainly retain the original character they have in the separated reactant species. Thus, **TS(1a→1b)/s** can be considered a product-like TS and **TS(1a→1b)/t** a reactant-like.

Table 3 gathers the energies of first-order saddle points involved in the three suggested mechanisms for the formation of epoxide. **TS(1a→1b)/t** is found to be only 4.8 kcal/mol less stable than **TS(1a→1b)/s**, and 34.8 kcal/mol above the reactants species. Further exploration of the PES shows that the crossing point might be located on the reactant side of the reaction path. Under these circumstances, the real TS for the reaction **1a→1b** cannot be directly taken as either **TS(1a→1b)/s** or **TS(1a→1b)/t**. Thus, it is only possible to estimate an upper bound to the energy of the actual TS from the crossing point where the two PESs merge. To locate this crossing point, IRC calculations have been performed (i) from **TS(1a→1b)/t** to the products, and (ii) from **TS(1a→1b)/s** to the reactants, Fig. 4.

The crossing point was located on the singlet PES immediately before **TS(1a→1b)/s** is reached from the reactant side. In the region where the two PESs intersect, the molecular geometries from the two reaction paths are very similar. It means that the activation barrier for the reaction **1a→1b** corresponds closely to the amount of energy required to surmount **TS(1a→1b)/s** (+30.0 kcal/mol, Fig. 2). Since it is the singlet TS that governs the reaction path from the reactant side, the oxygen-transfer process is not concerted: the two

Fig. 2. Reaction profile of the three suggested mechanisms for the formation of epoxide precursor from the addition of CrO_2Cl_2 to ethylene. Energies (in kcal/mol) are relative to singlet **1a**.

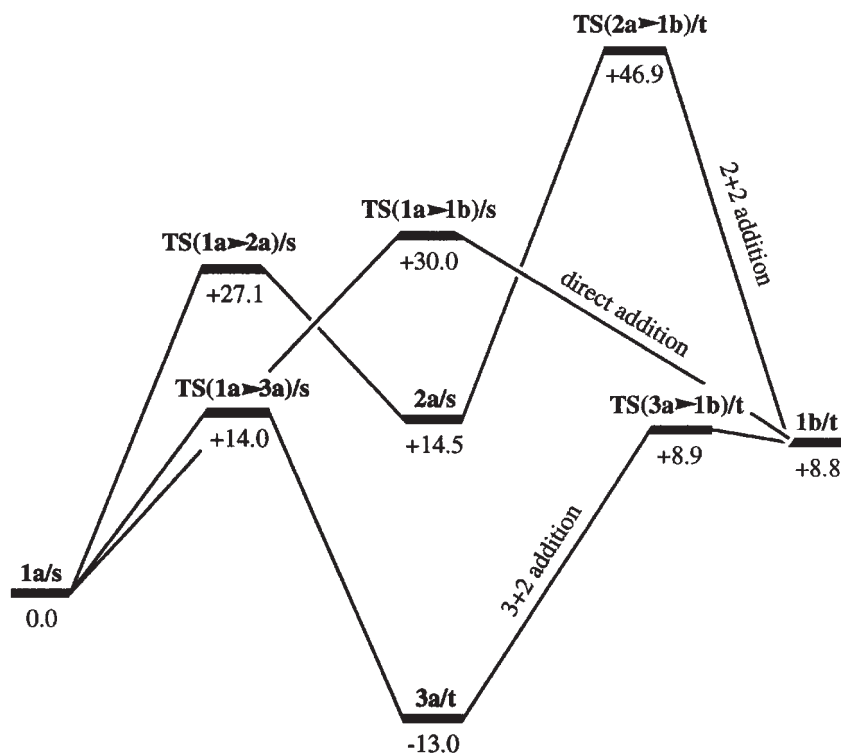
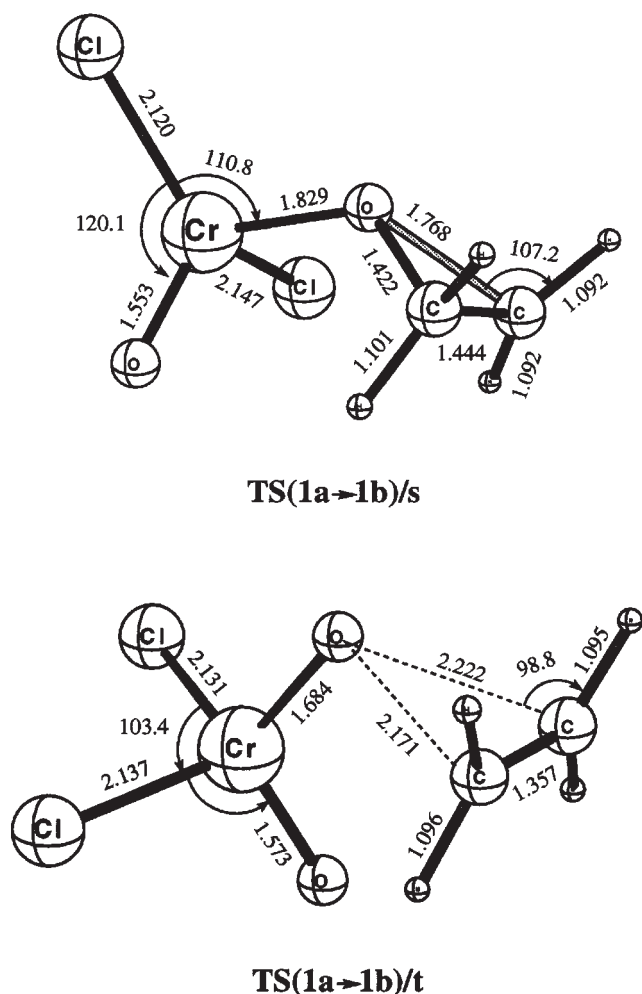


Fig. 3. Optimized geometrical parameters of the two possible transition state structures involved in the mechanism of direct addition for the formation of epoxide precursor. Distances in Å, and angles in degrees.



emerging C—O bonds are quite dissimilar (1.422 and 1.768 Å) in **TS(1a→1b)/s** (Fig. 3). Once the maximum has been reached on the singlet PES, the reaction can proceed along the triplet PES while the energy keeps decreasing until species **1b** is formed. The crossing from the singlet to the triplet PESs can be facilitated under the adiabatic assumption (42) by spin-orbit coupling.

Let us turn now our attention to the mechanism by postulated Sharpless et al. (5) involving a [2+2] interaction. The initial step was suggested to be the formation of a chromyl chloride olefin π complex. Despite looking for such a complex, we have not been able to localize any minimum on the PES close to the reactants region. This notwithstanding, its existence cannot be definitively ruled out, keeping in mind the well-known difficulties for DFT methods to describe weak interactions (43).

From that hypothetical complex, a four-centered intermediate **2a** was postulated to be formed via a [2+2] interaction between the olefin and an oxo group on the chromium (5). Indirect support for this process was provided by means of similar reported examples involving block-*p* elements (44).

Table 3. Energies^a (in kcal/mol) and imaginary frequencies (in cm^{-1}) of all first-order saddle points involved in the three suggested mechanisms for the formation of the epoxide precursor (s = singlet, t = triplet).

TS	ν^{\ddagger}	Energy
TS(1a→1b)/s	385.6i	30.0
TS(1a→1b)/t	229.5i	34.8
TS(1a→2a)/s	394.6i	27.1
TS(2a→1b)/s	555.0i	46.9
TS(2a→1b)/t	406.6i	31.4
TS(1a→3a)/s	363.8i	14.0
TS(1a→3a)/t	220.3i	21.7
TS(3a→1b)/t	27.4i	8.9

^aEnergies relative to free $\text{CrO}_2\text{Cl}_2 + \text{C}_2\text{H}_4$.

The optimized geometry of intermediate **2a**, together with the corresponding TSs of the whole [2+2] path are sketched in Fig. 5.

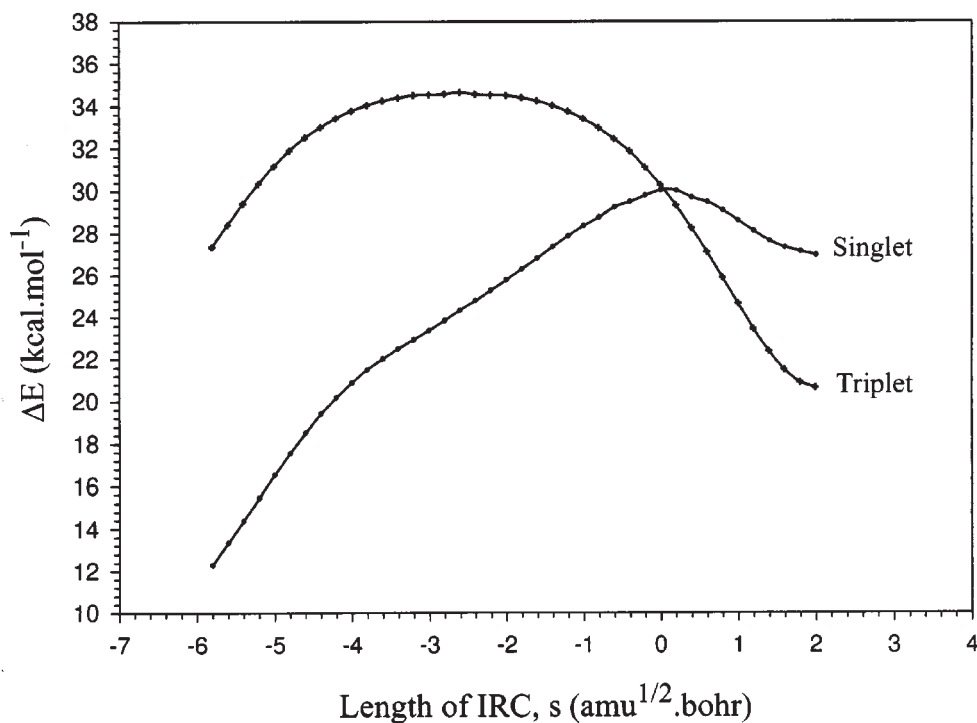
No change of the PES occurs in the reaction step **1a**→**2a**, since both reactants and product have singlet ground states. In contrast, the crossing takes place in the step **2a**→**1b**. The first step, **1a**→**2a**, turns out to be endothermic by 14.5 kcal/mol, and has an activation barrier of 27.1 kcal/mol (Fig. 2). The high energy required to reach **TS(1a→2a)** mainly arises from the Cr—O and C=C bond-breaking processes, which are slightly ahead of the bond-making ones (Fig. 5). This value is close to the 24.6 kcal/mol energy barrier found for the $[2\sigma+2\pi]$ attack between CrO_2Cl_2 and CH_3OH (32c). Remarkably, the corresponding [2+2] addition involving OsO_4 has been found to have an even higher energy barrier of 39.7 kcal/mol (45a).

Regarding the second step, it is found to be slightly exothermic (−5.7 kcal/mol), with an activation barrier as high as 46.9 kcal/mol (Fig. 2). By inspection of Fig. 5, such an energy-demanding barrier can be mainly ascribed to the strain around the oxygen atom in the four-center kite-shaped **TS(2a→1b)**. Also the loss of the Cr-C σ interaction is a destabilizing factor.

We have tentatively (Fig. 2) assigned **TS(2a→1b)/t** as the transition state for the second rearrangement step, since it lies 15.5 kcal/mol below **TS(2a→1b)/s**. According to Fig. 5, **TS(2a→1b)/s** is ahead of **TS(2a→1b)/t** along the reaction coordinate from **2a/s** to **1b/t**. It means that there are two different possibilities for the crossover to occur: (i) at the early stages of the reaction, prior to any of the two TSs, or (ii) still in the reactant-side of the reaction, but between the two TSs. Only in the former case the true TS governing the reaction step is **TS(2a→1b)/t** (as depicted in Fig. 2). If the crossover took place between the two TSs, then the highest point in energy in the step **2a**→**1b** would not correspond to **TS(2a→1b)/t** but to the crossing point of the two surfaces, and the barrier would be somewhat lower than the reported 46.9 kcal/mol. This second possibility cannot be discarded. However, it is clear from Fig. 2 that the structures of the two TSs are similar enough to ensure that the crossing point would not be far away in energy from **TS(2a→1b)/t**.

Up to this point, none of the two presented mechanisms seems to afford a low-energy path to the epoxide precursor **1b**. A third alternative for the reaction to proceed is via a [3+2] cycloaddition. Figure 6 shows the optimized geome-

Fig. 4. Energy profile for the reaction involving direct addition of CrO_2Cl_2 to ethylene along the IRC path in the region where the crossing between the two PESs occurs. The TS in the singlet surface is at $s = 0.0$, and the TS in the triplet surface at $s = -2.6$. Energies (in kcal/mol) are relative to singlet **1a**.



tries of the main stationary points corresponding to the [3+2] mechanism. The activation barriers for the two-step process involving a [3+2] interaction are +14.0 kcal/mol for the **1a**→**3a** reaction step (for the same OsO_4 -catalyzed process (45), the energy barrier is 1.8 kcal/mol), and 21.9 kcal/mol for the **3a**→**1b** reaction step. The former step involves a crossover from the singlet surface in **1a** to the triplet surface in **3a** (Table 2). Such a crossover has been analyzed in detail in a previous study by means of IRC calculations (46). It has been found that the crossing point is located in the product side of the reaction path, the corresponding **TS(1a**→**3a)** lying on the singlet surface. Should this crossing be made possible by spin-orbit coupling (42), nothing seems to prevent the **1a**→**3a** reaction step from being kinetically feasible. From a thermodynamic viewpoint, this process is found to be exothermic (−13.0 kcal/mol), and therefore also very favorable.

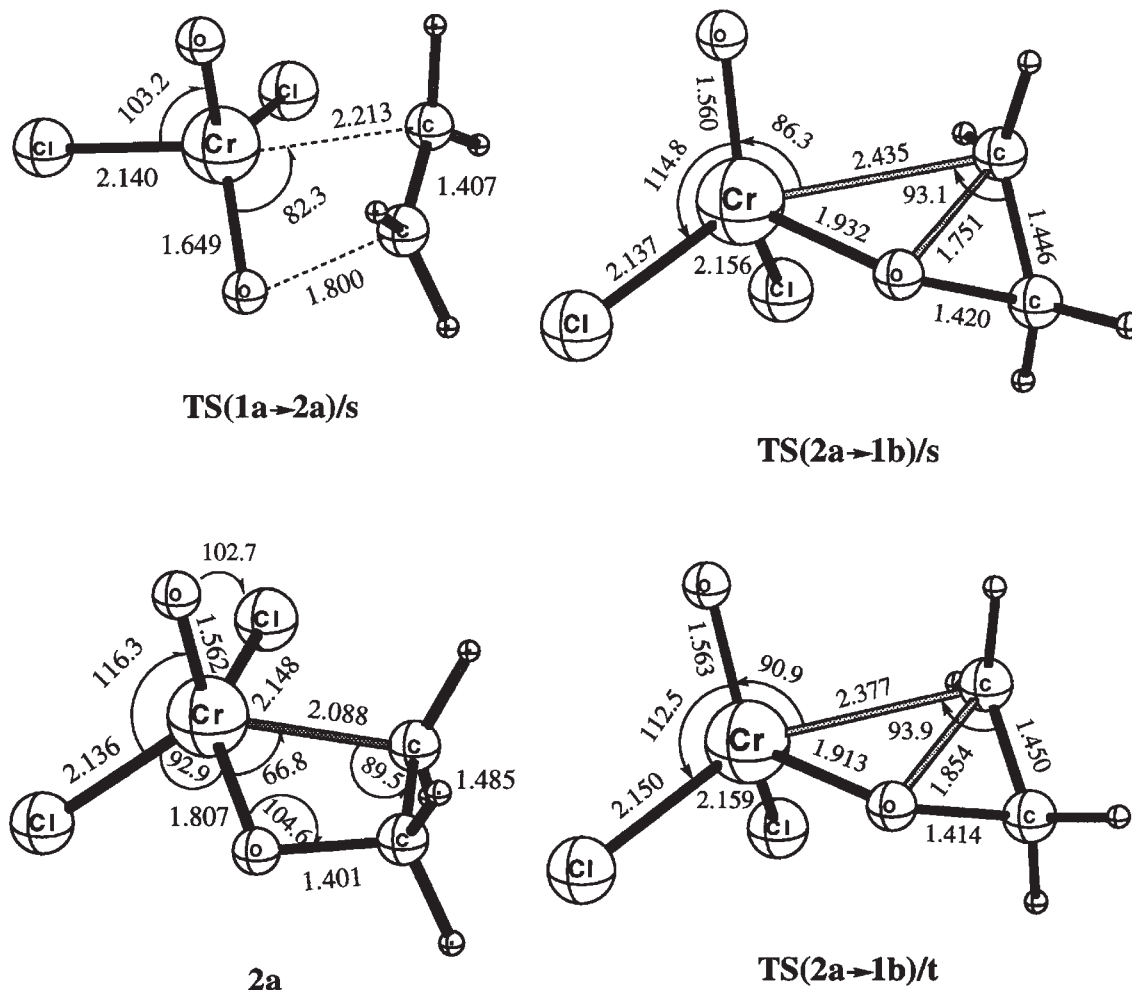
As seen from Fig. 6, the TS for the second reaction step, **3a**→**1b**, resembles very much intermediate **1b**. For instance, the geometry of the $\text{O}(\text{CH}_2)_2$ skeleton in this product-like TS is very close to the geometrical arrangement found in the precursor of the epoxide (Fig. 1). This is consistent with the fact that **TS(3a**→**1b)** is only 0.1 kcal/mol above **1b** (Fig. 2). Also notice the low value of the unique imaginary frequency for this TS (Table 2), which is indicative of a flat region.

It follows from the previous discussion that the most suitable path leading to the epoxide precursor **1b** is through [3+2] cycloaddition. The [3+2] addition of ethylene to CrO_2Cl_2 has a relatively low activation barrier of 14.0 kcal/mol, as the occupied π -orbital of ethylene can interact, stabilizing with the CrO_2Cl_2 LUMO throughout the

reaction (46). Further, the resulting five-membered ring, **3a/t**, is sufficiently flexible to allow for a facile rearrangement route to the epoxide product **1b/t** with the transition state being only 8.9 kcal/mol above the separated reactants. We note that the recent photochemical matrix isolation study by Limberg and Köppe (53) found complexed epoxides to be formed by CrO_2Cl_2 whereas they found no evidence for the formation of a dioxylate. This, however, does not contradict our theoretical result that, on the ground-state potential energy surface, complexed epoxide can easily rearrange to the dioxylate with a barrier of 0.1 kcal/mol. As the authors pointed out, “the PES investigated in the matrix experiments under photolytic conditions is probably different from the one the system moves on when the reactions are induced thermally. Light of the wavelength 411 nm is far below the $\text{Cr}=\text{O}$ dissociation threshold so that CrO_2Cl_2 , which shows a visible absorption band nearby, takes up energy via this transition to reach an excited state capable of reacting with olefins under matrix conditions. Consequently the first transition states and intermediate geometries which have to be passed will be different from the thermal ones” (53).

In contrast to the [3+2] path, the [2+2] addition has a sizable barrier of 27.1 kcal/mol due to (46) the poor overlap between the occupied π -orbital of ethylene and the LUMO of CrO_2Cl_2 . It is as a consequence not likely to be the first step in the epoxidation process. Also, the further rearrangement of chromaoxetane, **2a/s**, leads to a strained transition state, **TS(2a**→**1b)/t** with a large estimated barrier of 31.4 kcal/mol. Finally, the direct [1+2] addition is also hampered by poor initial interaction between ethylene and CrO_2Cl_2 , leading to a prohibitive barrier of 30.0 kcal/mol.

Fig. 5. Optimized geometrical parameters of the main stationary points (minima and first-order saddle points) for the mechanism involving a [2+2] cycloaddition between CrO_2Cl_2 and ethylene for the formation of epoxide precursor. Distances in Å, and angles in degrees.



Similar conclusions have been drawn recently with regard to the relative feasibility of [2+2] and [3+2] addition for the osmium-catalyzed hydroxylation of olefins (41, 45, 47, 48). Our results contradict previous findings by Rappé et al. (8). In that work, the [3+2] path was ruled out because it was found to be strongly endothermic (+56 kcal/mol), whereas the [2+2] path was concluded to be exothermic (-14 kcal/mol) and actually the only one capable of yielding epoxide. However, that work was hampered by the lack of fully optimized structures. Also, Rappé et al. (8) find the reaction $\text{CrCl}_2\text{O}_2 + \text{C}_2\text{H}_4 \rightarrow \text{CrCl}_2\text{O} + \text{C}_2\text{H}_4\text{O}$ to be exothermic by -35 kcal/mol whereas our DFT method and experiment find it to be endothermic by 26.7 kcal/mol and 24.8 kcal/mol, respectively.

The assumed epoxide precursor **1b/t** does not readily decompose into epoxide. In fact, we calculate the reaction $\mathbf{1b/t} \rightarrow \text{CrCl}_2\text{O} + \text{C}_2\text{H}_4\text{O}$ to be endothermic by 16.9 kcal/mol, in keeping with the fact that the overall reaction $\text{CrCl}_2\text{O}_2 + \text{C}_2\text{H}_4 \rightarrow \text{CrCl}_2\text{O} + \text{C}_2\text{H}_4\text{O}$ is calculated to be endothermic by 26.7 kcal/mol. Thus, the many mechanisms invoking **1b/t** (and an implied exothermicity for the overall reaction $\text{CrCl}_2\text{O}_2 + \text{C}_2\text{H}_4 \rightarrow \text{CrCl}_2\text{O} + \text{C}_2\text{H}_4\text{O}$) might not be valid.

We speculate that H_2O instead is involved in the formation of epoxide as the reaction mixture of Scheme 1 is extracted from an organic solvent (such as CH_2Cl_2) into aqueous solution. This possibility will be the subject of an upcoming investigation (45a).

It is worthwhile pointing out that dioxyolate complexes of Re and Os are both known and well characterized. Unlike the Cr system, these complexes are known to hydrolyze to *cis* diols rather than epoxides. This can be understood because both the Re and Os system contain only oxygen ligands whereas the Cr system involves both oxygen and chlorine ligands.

III.2. Formation of the chlorohydrin precursor

The conversion of olefins into chlorohydrins was originally suggested to result from highly stereoselective *cis* addition of the elements of HOCl across the olefinic linkage (5). Chlorohydrins resulting from *trans* addition were concluded to be secondary products derived by opening of the epoxide (5). According to Scheme 2, *cis*-oxychlorination can be accounted for by two different mechanistic routes: inter-

Fig. 6. Optimized geometrical parameters of the main stationary points (minima and first-order saddle points) for the mechanism involving a [3+2] cycloaddition between CrO_2Cl_2 and ethylene for the formation of epoxide precursor. Distances in Å, and angles in degrees.

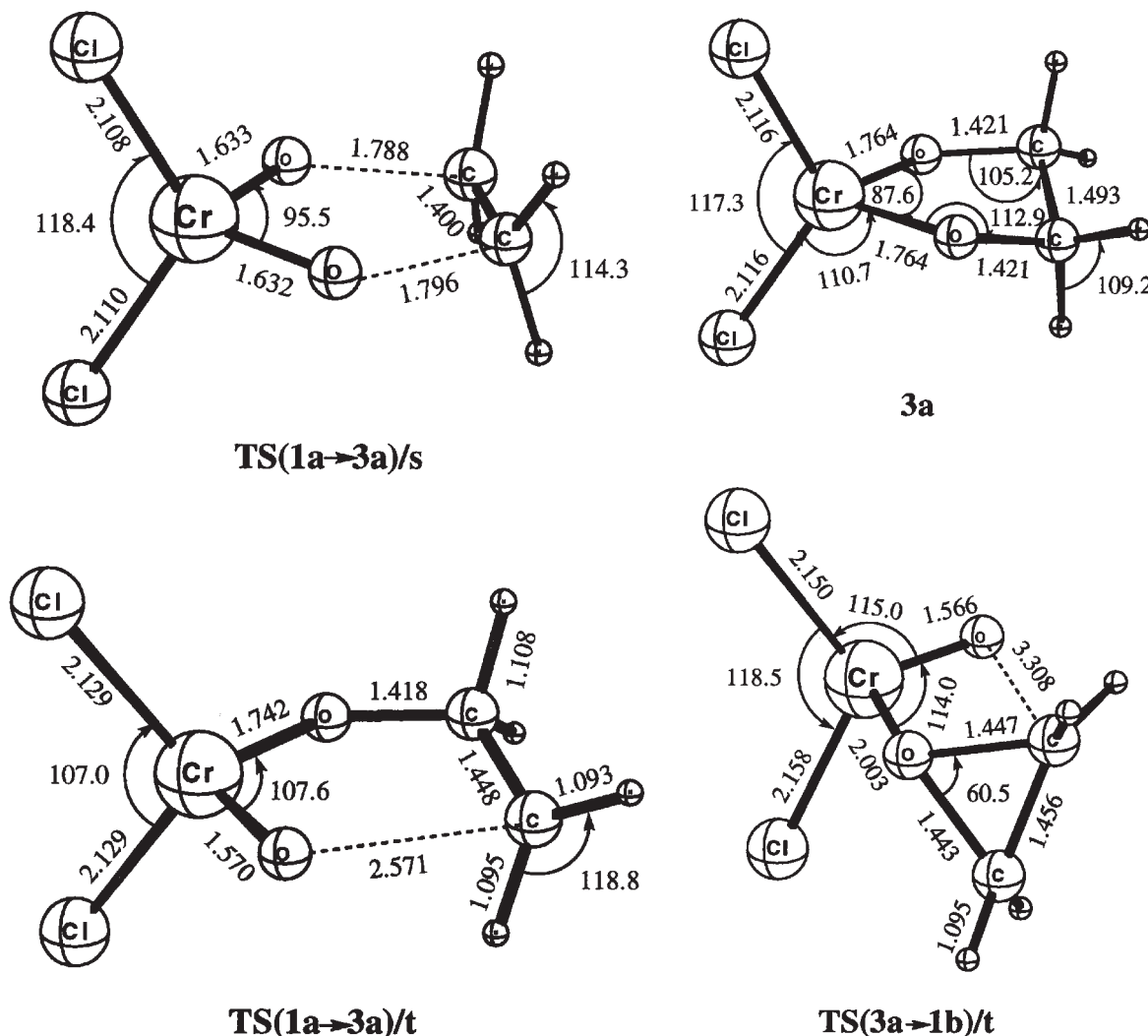


Table 4. Energies^a (in kcal/mol) of all minima involved in the suggested mechanisms for the formation of chlorohydrin and dichloride precursors (s = singlet, t = triplet).

Minima	Ground state	Energy
4a	s	7.6
5a	t	3.8
6a	t	44.7

^aEnergies relative to free $\text{CrO}_2\text{Cl}_2 + \text{C}_2\text{H}_4$.

mediate **5a** (the immediate precursor of 1,2-chlorohydrin) can be thought to derive from either a [2+2] addition (center) or a [3+2] addition (left).

In the mechanism involving a [2+2] cycloaddition, the formal transfer of O and Cl from CrO_2Cl_2 to ethylene occurs in two separated steps, whereas in the [3+2] mechanism the two heteroatoms are transferred in the same reaction step. As far as the [2+2] route is concerned, there are even two different possibilities for the reaction to proceed, depending on the relative order by which the heteroatoms are inserted:

(i) insertion of Cl in the first step, then O, or (ii) first O, then Cl. Only the former possibility has been depicted in Scheme 2. The latter possibility would mean that, instead of intermediate **4a**, the product obtained after the first reaction step would be the highly energetic chromaoxetane **2a**, whose endothermic formation has been already discussed in the previous section; afterwards, the second step would be a bond migration between **2a** and **5a**. We will come to this point later on.

Tables 4 and 5 gather relevant information concerning all the stationary points involved in the mechanisms for the CrO_2Cl_2 -mediated formation of chlorine-containing products from ethylene. Notice that the immediate precursor of 1,2-chlorohydrin, **5a**, lies on the triplet surface in its ground state, whereas **4a** is more stable on the singlet surface. To ensure that these conformations (Fig. 7) are the more stable ones, we also examined three other conformers in which the ligands that do not participate in the ring adopt different orientations. All the isomers were found to be very close in energy to **4a** and **5a** (higher by only 0.1–0.9 kcal/mol). The

Table 5. Energies^a (in kcal/mol) and imaginary frequencies (in cm⁻¹) of all first-order saddle points involved in the suggested mechanisms for the formation of chlorohydrin and dichloride precursors (s = singlet, t = triplet).

TS	ν^-	Energy
TS(1a→4a)/s	52.0i	9.1
TS(1a→5a)/s	131.3i	15.7
TS(1a→5a)/t	69.4i	37.3
TS(4a→5a)/s	532.7i	49.8
TS(4a→5a)/t	121.7i	50.5

^aEnergies relative to free CrO₂Cl₂ + C₂H₄.

differences are so small that those species must be thought to coexist and easily interconvert between each other during the reaction.

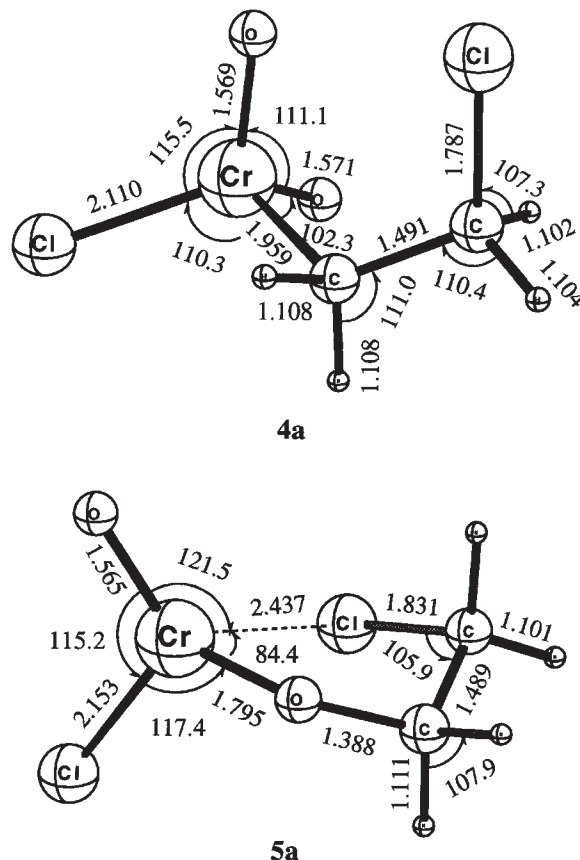
The relative energies and activation barriers for the two pathways leading to chlorohydrin are summarized in Fig. 8. Figures 9 and 10 display the molecular structures of the TSs corresponding to the [2+2] and [3+2] mechanisms, respectively. The [2+2] attack of ethylene on the Cr—Cl bond (Fig. 8) has an energy barrier (9.1 kcal/mol), which is only one third of the barrier corresponding to the same attack on the Cr=O bond (Fig. 2).

However, as can be seen from Fig. 8, the whole [2+2] pathway cannot compete in energy with the [3+2] path. In particular, the main bottleneck for the former route happens to take place in the second step. The conversion of **4a** to **5a**, despite being formally exothermic ($\Delta E = -3.8$ kcal/mol), is kinetically prevented ($\Delta E^\ddagger = +49.8$ kcal/mol). Indeed, the TS connecting **4a** and **5a** (either singlet or triplet) suffers from substantial constraint due to the tight three-membered ring formed during the transfer of the second heteroatom (one O atom in this case) to the organic skeleton. It can be inferred that, if the second heteroatom to be transferred was Cl instead of O (as it would occur in the bond migration **2a**→**5a**), similar constraints would be also responsible for the strain and, therefore, for the large amount of energy required for this process to take place.

Complex **5a/t** (ground state) is computed to lie 10.2 kcal/mol below **5a/s** (first excited state). According to our calculations, the alternative [3+2] cycloaddition reaction should proceed from **1a** to **5a/t** in a single step involving a change of the PES. Notice from Fig. 10 that TS(1a→5a)/s is slightly ahead of TS(1a→5a)/t. The crossing point is expected to be found somewhere between the two TSs, and much closer to TS(1a→5a)/s than to TS(1a→5a)/t, since the latter lies 21.6 kcal/mol above the former. In principle, one could make a rough approximation and assume that the crossover occurs at TS(1a→5a)/s (as foreseen for the **1a**→**1b** step). In this way, the barrier assigned to the **1a**→**5a** step (+15.7 kcal/mol) should be better considered as an upper bound to the real activation barrier. Strictly speaking, the crossing point might not coincide with the singlet TS. The closer the two points, the more valid the approximation. However, even in the case that the crossing point happened to occur much earlier than TS(1a→5a)/s, the global result would not be significantly affected because the trend is in the direction of making the barrier even smaller.

Taking into account such an assumption, notice from Fig. 10 that TS(1a→5a)/s does not suffer from much distur-

Fig. 7. Optimized geometrical parameters of intermediate **4a** and ester **5a** derived, respectively, from a [2+2] addition of ethylene to one Cr—Cl bond, and from a [3+2] addition of ethylene to one Cr—Cl bond and one Cr=O bond in CrO₂Cl₂. Distances in Å, and angles in degrees.



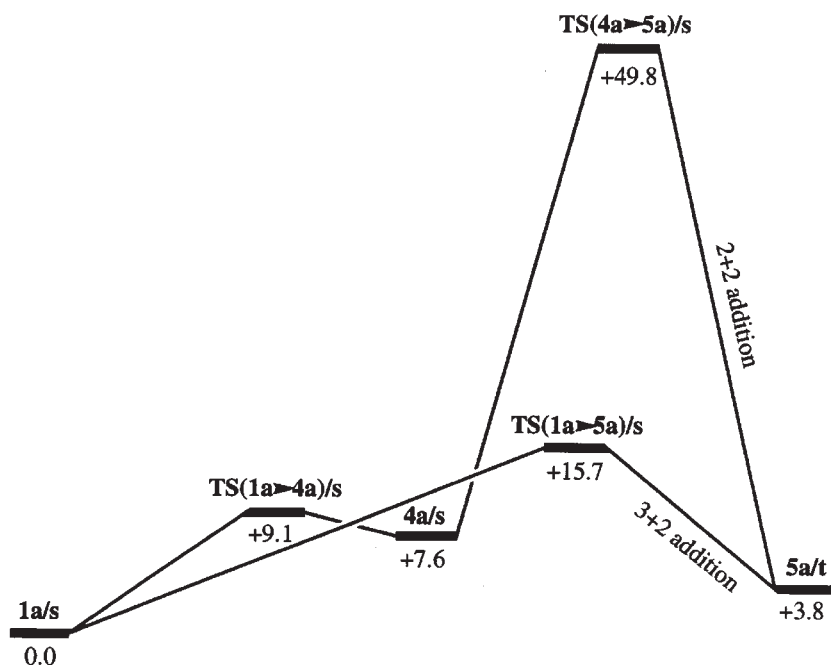
tion. The most remarkable point is the closing of the ClCrO bond angle (89.2°) in order to better assist the olefin attack, which proceeds coplanar to the Cl-Cr-O plane (dihedral angle Cl-C-C-O = 2.2°). Once in the product side, the reaction is predicted to proceed smoothly along the triplet PES.

Weighing up both mechanisms, the [2+2] cycloaddition proves less beneficial to the energetics of *cis*-oxygenchlorination than the [3+2], regardless of the relative order by which the two heteroatoms are inserted. Consequently, it can be concluded that the mechanism that actually operates in the formation of the chlorohydrin precursor (**5a/t**) from the addition of ethylene to CrO₂Cl₂ is the one involving the direct formation of the five-membered intermediate **5a/t** from a [3+2] addition.

We have previously shown (45a) that the [3+2] addition of ethylene to two Cr=O bonds has a low barrier due to stabilizing interactions between the LUMO of CrO₂Cl₂ and the occupied ethylene π -orbital. Quite similar interactions are operative for the [3+2] addition of ethylene to, respectively, a Cr=O and Cr—Cl bond. It is thus not surprising that the two types of [3+2] addition have nearly the same activation energies.

The final formation of chlorohydrin from **5a/t** requires a hydrogen agent. We speculate again that H₂O is involved as

Fig. 8. Reaction profile of the two possible mechanisms for the formation of 1,2-chlorohydrin precursor from the addition of CrO_2Cl_2 to ethylene. Energies (in kcal/mol) are relative to **1a**.



the reaction mixture of Scheme 2 is extracted from an organic solvent (such as CH_2Cl_2) into aqueous solution. Thus, the reaction of H_2O with **5a/t** to produce $\text{Cr}(\text{OH})\text{OCl}/\text{t}$ + chlorohydrin is calculated to have a modest endothermicity of 2.4 kcal/mol. We shall examine this step in an upcoming investigation.²

III.3. Dichloride formation

Chromyl chloride oxidations of olefins are known to produce complex mixtures of products (1). However, it was found that when these reactions are performed at low temperature the epoxide and the chlorohydrin become the major products. Only in a few cases does *cis*-dichlorination really occur (5). According to Scheme 2, formation of dichloride may proceed through two different reaction pathways. Again, either a [2+2] (center) or a [3+2] addition path (right) seem conceivable modes of reaction. In the former case, ethylene may insert into a chlorine–chromium bond (*cis*-chlorometalation) to produce the alkylchromium intermediate **4a**. Such a process has been already analyzed in the previous section. This species could then lead to the precursor of dichloride, **6a**, by reductive elimination in the second step. The first step, however, has to occur with retention of configuration at the carbon center bound to the chromium in **4a** in order to result in overall *cis* addition. Alternatively, the two chlorine atoms may be transferred in a one-step process.

Figure 11 shows the optimized geometry of the immediate precursor of dichloride, **6a**. This can be considered a five-membered species such as **3a** and **5a**. However, notice that, unlike in **3a** and **5a**, the five atoms of the ring in intermediate **6a** are not coplanar. This conformation ensures the optimal interaction between ethylene π -orbital and the LUMO of

CrO_2Cl_2 . The energetics of the reaction leading to dichloride is summarized in Fig. 12. The most remarkable point here is the high endothermicity of the net reaction (+44.7 kcal/mol), which prevents dichloride formation from being favored at low temperatures. Since already the thermodynamics makes dichloride formation prohibitive under normal condition, the TSs involved in the path from **1a** to **6a** have not been investigated.

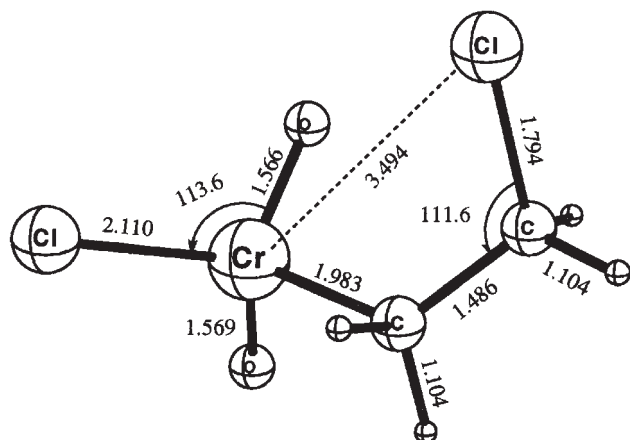
To sum up, comparison of Figs. 2, 8, and 12 allows us to conclude that the formation of dichloride, regardless of the mechanistic path being followed, cannot compete energetically with the formation of either epoxide or chlorohydrin. Our calculations reveal that, thermodynamically, *cis*-dichlorination is more unlikely to occur than any other of the processes leading to the observed products.

III.4. Dependence of the reaction mechanism on the organic substrates

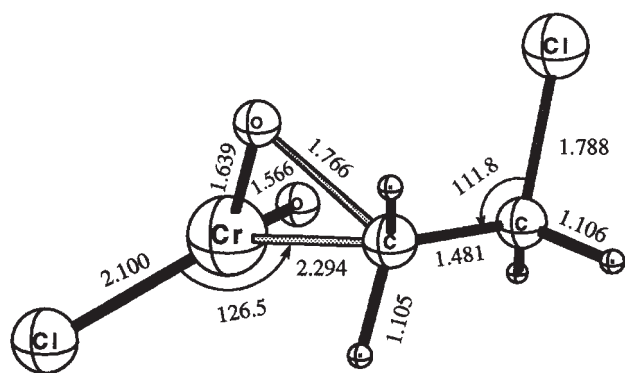
We shall finally briefly discuss changes of relative energies and possibly the reaction mechanism when considering olefins other than ethylene. Table 6 compares the reaction enthalpies for the formation of diolate and epoxide complexes as well as the fully separated epoxides from reaction between CrCl_2O_2 and the two olefins cyclohexene and tetramethyl ethylene. It follows from Table 6 that, although the relative energies change to a certain extent when the organic substrates changes, the main conclusions drawn from the discussion for oxidation of ethylene remain the same. That is, (i) diolate is the most stable complex in all cases; (ii) difference in relative energies between the diolate and epoxide complexes are substantial; and (iii) oxidation of olefin to the separated epoxide is highly endothermic. We

²M. Torrent, L. Deng, M. Solà, and T. Ziegler. Work in progress.

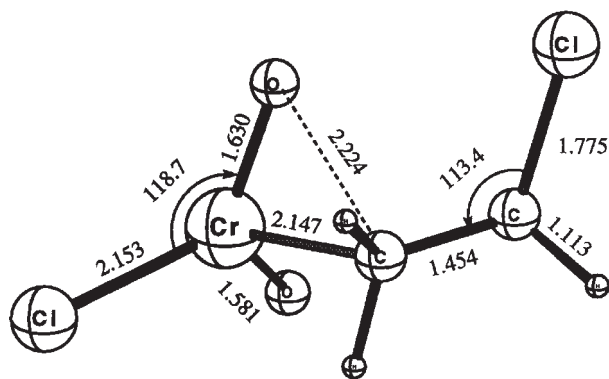
Fig. 9. Optimized geometrical parameters of the transition state structures involved in the [2+2] cycloaddition between CrO_2Cl_2 and ethylene leading to the formation of chlorine-containing products. Distances in Å, and angles in degrees.



TS(1a→4a)/s

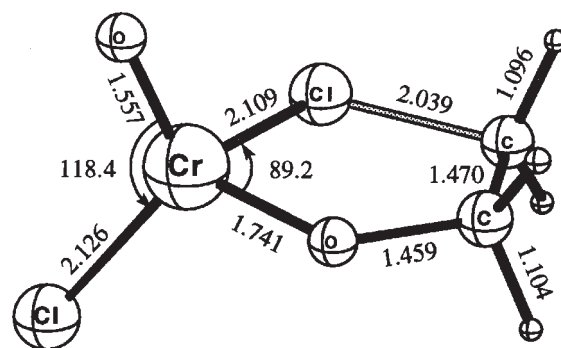


TS(4a→5a)/s

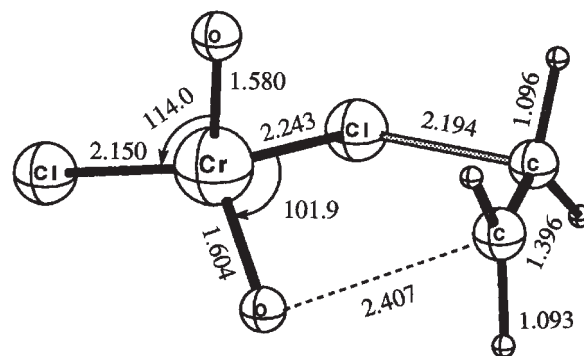


TS(4a→5a)/t

Fig. 10. Optimized geometrical parameters of the transition state structures involved in the [3+2] cycloaddition between CrO_2Cl_2 and ethylene leading to the formation of 1,2-chlorohydrin precursor. Distances in Å, and angles in degrees.

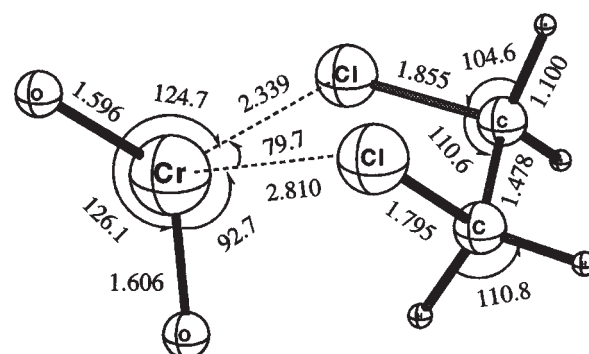


TS(1a→5a)/s



TS(1a→5a)/t

Fig. 11. Optimized geometrical parameters of the immediate precursor of 1,2-dichloride. Distances in Å, and angles in degrees.



6a

Fig. 12. Reaction profile for the formation of 1,2-dichloride precursor from the addition of ethylene to CrO_2Cl_2 . Energies (in kcal/mol) are relative to **1a**.

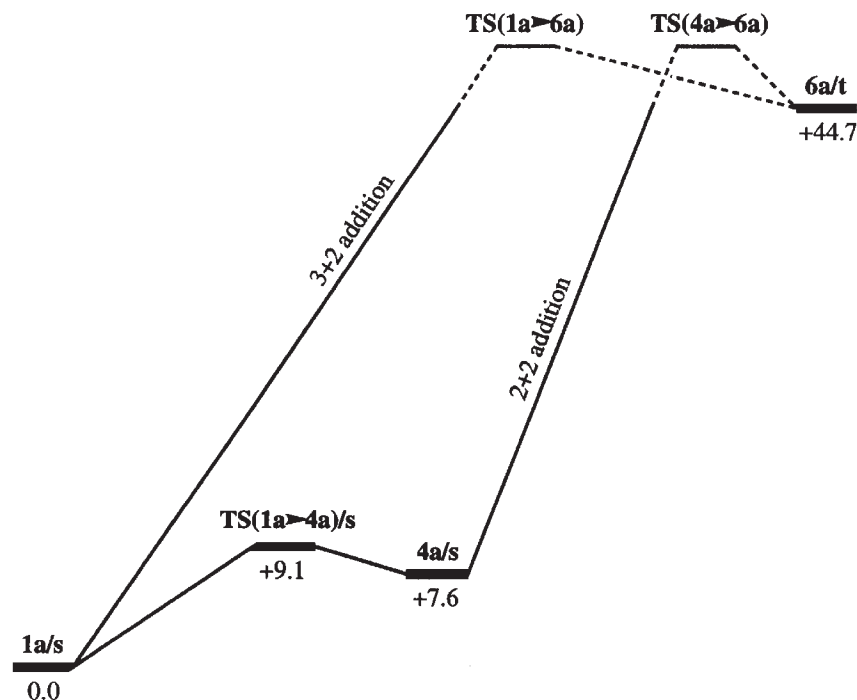


Table 6. Comparison of reaction enthalpies of the oxidation of olefin by CrO_2Cl_2 to chromyl diolate and epoxide complexes for different olefins.

Reaction ^a	Energy ^b (kcal/mol)	ΔE^c (kcal/mol)
$\text{CrO}_2\text{Cl}_2 + \text{C}_2\text{H}_4 \rightarrow \text{CrCl}_2(\text{OCH}_2\text{CH}_2\text{O})$	-13.0 (-10.6 ^d)	0
$\text{CrO}_2\text{Cl}_2 + \text{C}_2\text{H}_4 \rightarrow \text{CrCl}_2(\text{O})(\text{OCH}_2\text{CH}_2)$	8.6	21.6
$\text{CrO}_2\text{Cl}_2 + \text{C}_2\text{H}_4 \rightarrow \text{CrOCl}_2 + \text{epoxide}$	26.7	39.7
$\text{CrO}_2\text{Cl}_2 + \text{C}_2\text{Me}_4 \rightarrow \text{CrCl}_2(\text{OCMe}_2\text{CMe}_2\text{O})$	-19.5	0.0
$\text{CrO}_2\text{Cl}_2 + \text{C}_2\text{Me}_4 \rightarrow \text{CrCl}_2(\text{O})(\text{OCMe}_2\text{CMe}_2)$	-4.8	14.7
$\text{CrO}_2\text{Cl}_2 + \text{C}_2\text{Me}_4 \rightarrow \text{CrOCl}_2 + \text{tetramethylethylene epoxide}$	3.7	23.2
$\text{CrO}_2\text{Cl}_2 + \text{cyclohexene} \rightarrow \text{Cr}(\text{O})(1,2\text{-cyclohexanediolate})$	-12.4	0.0
$\text{CrO}_2\text{Cl}_2 + \text{cyclohexene} \rightarrow \text{Cr}(\text{O})(1,2\text{-cyclohexene epoxide})$	5.9	18.3
$\text{CrO}_2\text{Cl}_2 + \text{cyclohexene} \rightarrow \text{CrOCl}_2 + \text{cyclohexene epoxide}$	30.0	42.4

^aThe BP86 calculations show that all the reactants have singlet ground state and all the products have triplet ground state.

^bUnless otherwise specified, the BP86 calculations were carried out with double- ζ basis set plus polarization (the standard ADF basis set III/H, C.1s, O.1s, Cl.2p) for nonmetal atoms, and triple- ζ basis set (the standard ADF basis set IV/Cr.2p) for Cr atom.

^cEnergy difference relative to the diolate complexes for each different organic substrates, respectively.

^dThe ADF calculations were performed with triple- ζ plus 3d and 4f polarization functions for C and Cl atoms, triple- ζ plus 2p and 3d polarization functions for H, and triple- ζ plus two 4f functions for Cr; the basis set for the nonmetals was taken from standard ADF basis set V, and the basis set IVB of ref. 49 was used for Cr atom.

therefore conclude that the mechanistic picture drawn from ethylene is not likely to change qualitatively with other olefins.

IV. Conclusions

We have shown that the formation of the reputed epoxide intermediate **1b/t** from the reaction between CrO_2Cl_2 and ethylene is unlikely to involve a chromaoxetane intermediate derived from a [2+2] cycloaddition as previously assumed (5). Our calculations reveal that the [3+2] addition of ethylene to chromium–oxygen bonds in CrO_2Cl_2 is favored over

the [2+2] addition to a Cr=O linkage, and also over the direct addition of ethylene to one oxygen atom. It is concluded that epoxides originate from an ester intermediate, which in turn is formed via a [3+2] cycloaddition.

We also suggest that chlorohydrin, the other major product observed in the oxidation of olefins by CrO_2Cl_2 , should arise from a [3+2] cycloaddition as well, in particular from the addition of ethylene to two different heteroatoms in the chromium reagent. Our theoretical results do not support an alternative two-step mechanism involving a [2+2] addition followed by a bond migration. Such a process is found to be too demanding in terms of energy, especially as far as the

activation barrier for the second step is concerned. In addition, the present investigation justifies why only in some cases dichloride is found among the observed products. Dichlorination is computed to be thermodynamically far less favorable than either epoxidation or oxychlorination as a product.

The decomposition of the reputed epoxide precursor **1b/t** into the final product (**1b/t** \rightarrow $\text{CrCl}_2\text{O} + \text{C}_2\text{H}_4\text{O}$) was found to be endothermic by 16.9 kcal/mol, in keeping with the fact that the overall reaction $\text{CrCl}_2\text{O}_2 + \text{C}_2\text{H}_4 \rightarrow \text{CrCl}_2\text{O} + \text{C}_2\text{H}_4\text{O}$ is calculated to be endothermic by 26.7 kcal/mol. Thus, the many mechanisms invoking **1b/t** (and an implied exothermicity for the overall reaction $\text{CrCl}_2\text{O}_2 + \text{C}_2\text{H}_4 \rightarrow \text{CrCl}_2\text{O} + \text{C}_2\text{H}_4\text{O}$) might not be valid. We plan in an upcoming investigation² to study the role of H_2O (or H^+/OH^-) for the formation of epoxide as the reaction mixture of Scheme 1 is extracted from an organic solvent (such as CH_2Cl_2) into aqueous solution. This investigation should also explain why diols are absent as products in the reaction between CrCl_2O_2 and olefins whereas the corresponding reaction between OsO_4 and olefins generates exclusively diols with little epoxide as a product.

Acknowledgments

This investigation was supported by the Natural Sciences and Engineering Research Council of Canada (NSERC), and by the Donors of the Petroleum Research Fund, administered by the American Chemical Society (ACS-PRF No 31205-AC3), as well as by the Spanish DGICYT Project No. PB95-0762. We also acknowledge access to the computer facilities at the universities of Calgary and Girona. One of us (M.T.) thanks the Direcció General de Recerca de la Generalitat de Catalunya for financial help through a FI Fellowship.

References

- (a) S.J. Cristol and K.R. Eilar. *J. Am. Chem. Soc.* **72**, 4353 (1950); (b) R.A. Stairs, D.G.M. Diaper, and A.L. Gatzke. *Can. J. Chem.* **41**, 1059 (1963); (c) F. Freeman. *Rev. React. Species Chem. React.* **1**, 37 (1973); (d) A. Wahhab. Ph.D. thesis. University of Calgary, Calgary, 1987. (e) F.W. Bachelor and U.O. Cheriyan. *Can. J. Chem.* **50**, 4022 (1972).
- (a) F.A. Carey and R.J. Sundberg. *Advanced organic chemistry*. Plenum, New York, 359 (1977); (b) W.A. Nugent and J.M. Mayer. *Metal-ligand multiple bonds*. Wiley, New York, 248 (1988).
- (a) K.B. Wiberg (*Editor*). *Oxidation in organic chemistry*. Part A. Academic Press, New York, 1965. pp. 1–68; (b) M. Schröder. *Chem. Rev.* **80**, 187 (1980).
- (a) R.A. Walton. *Prog. Inorg. Chem.* **16**, 1 (1972); (b) J. San Filippo, Jr., and C. Chern. *J. Org. Chem.* **42**, 2182 (1977); (c) F. Freeman, C.R. Armstead, M.G. Essig, E.L. Karchefski, C.J. Kojima, V.C. Manopoli, and A.H. Wickman. *J. Chem. Soc. Chem. Commun.* **65** (1980).
- K.B. Sharpless, A.Y. Teranishi, and J.-E. Bäckvall. *J. Am. Chem. Soc.* **99**, 3120 (1977).
- F. Freeman. *Chem. Rev.* **75**, 439 (1975).
- E.G. Samsel, K. Srinivasan, and J.K. Kochi. *J. Am. Chem. Soc.* **107**, 7606 (1985).
- (a) A.K. Rappé and W.A. Goddard. *J. Am. Chem. Soc.* **102**, 5114 (1980); (b) *J. Am. Chem. Soc.* **104**, 3287 (1982); (c) T.H. Upton and A.K. Rappé. *J. Am. Chem. Soc.* **107**, 1206 (1985).
- A.K. Rappé and W.A. Goddard. *Nature (London)*, **285**, 311 (1980).
- (a) J.-E. Bäckvall, M.W. Young, and K.B. Sharpless. *Tetrahedron Lett.* **40**, 3523 (1977); (b) M.F. Schlecht and H.-J. Kim. *Tetrahedron Lett.* **27**, 4889 (1986); (c) M.F. Schlecht and H.-J. Kim. *J. Org. Chem.* **54**, 583 (1989).
- (a) D. Mansuy, J. Leclaire, M. Fontecave, and P. Dausette. *Tetrahedron*, **40**, 2847 (1984); (b) J.P. Collman, J.I. Brauman, B. Meunier, S.A. Raybuck, and T. Kodadek. *Proc. Natl. Acad. Sci. U.S.A.* **81**, 3245 (1984); (c) P.R. Ortiz de Montellano and E.A. Komives. *J. Biol. Chem.* **260**, 3330 (1985); (d) J.P. Collman, J.I. Brauman, B. Meunier, T. Hayashi, T. Kodadek, and S.A. Raybuck. *J. Am. Chem. Soc.* **107**, 2000 (1985); (e) J.T. Groves and Y. Watanabe. *J. Am. Chem. Soc.* **108**, 507 (1986); (f) E.A. Komives and P.R. Ortiz de Montellano. *J. Biol. Chem.* **262**, 9793 (1987).
- A.G.M. Barrett, D.H.R. Barton, and T. Tsushima. *J. Chem. Soc. Perkin Trans. 1*, 639 (1980).
- J.T. Groves and T.E. Nemo. *J. Am. Chem. Soc.* **105**, 5786 (1983).
- K. Yamaguchi, Y. Tekahara, and T. Fueno. *In Applied quantum chemistry*. Edited by V.H. Smith, H.F. Schaefer, and K. Morokuma. D. Reidel, Dordrecht, 155 (1986).
- (a) D.M. Walba, C.H. DePuy, J.J. Grabowski, and V.M. Bierbaum. *Organometallics*, **3**, 498 (1984); (b) H. Kang and J.L. Beauchamp. *J. Am. Chem. Soc.* **101**, 6449 (1979).
- K.A. Jørgensen and B. Schiøtt. *Chem. Rev.* **90**, 1483 (1990).
- (a) M.J. Calhorda, A.M. Galvão, C. Ünaleroğlu, A.A. Zlota, F. Frolow, and D. Milstein. *Organometallics*, **12**, 3316 (1993); (b) J. Bakos, Á. Orosz, S. Cserépi, I. Tóth, and D. Sinou. *J. Mol. Catal. A*, **116**, 85 (1997); (c) B. Bruin, M.J. Boerakker, J.J.J.M. Donners, B.E.C. Christiaans, P.P.J. Schlebos, R. Gelder, J.M.M. Smits, A.L. Spek, and A.W. Gal. *Angew. Chem. Int. Ed. Engl.* **36**, 2064 (1997); *Angew. Chem.* **109**, 2153 (1997).
- V.W. Day, W.G. Klemperer, S.P. Lockledge, and D.J. Main. *J. Am. Chem. Soc.* **112**, 2031 (1990).
- S. Baba, T. Ogura, and S. Kawaguchi. *J. Chem. Soc. Chem. Commun.* 910 (1972).
- M. Lenarda, N.B. Pahor, M. Calligaris, M. Graziani, and L. Randaccio. *J. Chem. Soc. Dalton Trans.* 279 (1978).
- (a) B.B. Ebbinghaus. *Combust. Flame*, **101**, 311 (1995); (b) C. Limberg, R. Köppe, and H. Schnöckel. *Angew. Chem.* **110**, 512 (1998).
- (a) E.J. Baerends, D.E. Ellis, and P. Ros. *Chem. Phys.* **2**, 41 (1973); (b) W. Ravenek. *In Algorithms and applications on vector and parallel computers*. Edited by H.J.J. te Riele, T.J. Dekker, and H.A. van de Vorst. Elsevier, Amsterdam, 1987.
- (a) P.M. Borrigger, G. te Velde, and E.J. Baerends. *Int. J. Quantum Chem.* **33**, 87 (1987); (b) G. te Velde and E.J. Baerends. *J. Comput. Phys.* **99**, 84 (1992).
- J. Krijn and E.J. Baerends. *Fit functions in the HFS-methods; internal report*. Free University of Amsterdam, Amsterdam, 1984.
- (a) G.J. Snijders, E.J. Baerends, and P. Vernooijs. *At. Nucl. Data Tables*, **26**, 483 (1982); (b) P. Vernooijs, G.J. Snijders, and E.J. Baerends. *Slater type basis functions for the whole periodic system; internal report*. Free University of Amsterdam, The Netherlands, 1981.
- (a) G.J. Snijders, E.J. Baerends, and P. Ros. *Mol. Phys.* **36**, 1789 (1978); (b) *Mol. Phys.* **38**, 1909 (1979).

27. O. Gunnarson and I. Lundquist. *Phys. Rev* **B10**, 1319 (1974).
28. S.H. Vosko, L. Wilk, and M. Nusair. *Can. J. Phys* **58**, 1200 (1980).
29. A.D. Becke. *Phys. Rev. A*, **38**, 2398 (1988).
30. (a) J.P. Perdew. *Phys. Rev. Lett* **55**, 1655 (1985); (b) *Phys. Rev. B: Condens. Matter*, **33**, 8822 (1986); (c) J.P. Perdew and Y. Wang. *Phys. Rev. B: Condens. Matter*, **33**, 8800 (1986).
31. M. Torrent, P. Gili, M. Duran, and M. Solà. *J. Chem. Phys.* **104**, 9499 (1996).
32. (a) L. Deng and T. Ziegler. *Organometallics*, **15**, 3011 (1996); (b) T. Ziegler and J. Li. *Organometallics*, **14**, 214 (1995); (c) L. Deng and T. Ziegler. *Organometallics*, **16**, 716 (1997).
33. (a) L. Versluis and T. Ziegler. *J. Chem. Phys* **88**, 322 (1988); (b) L. Fan and T. Ziegler. *J. Chem. Phys* **95**, 7401 (1991); (c) G. Schreckenbach, J. Li, and T. Ziegler. *Int. J. Quantum Chem.* **56**, 477 (1995).
34. L. Fan, L. Versluis, T. Ziegler, E.J. Baerends, and W. Ravenek. *Int. J. Quantum Chem. Symp.* **22**, 173 (1988).
35. A. Banerjee, N. Adams, J. Simons, and R. Shephard. *J. Phys. Chem* **89**, 52. (1985).
36. J. Baker. *J. Comput. Chem* **7**, 385 (1986).
37. L. Fan and T. Ziegler. *J. Chem. Phys.* **92**, 46 (1990).
38. K. Fukui. *Acc. Chem. Res.* **14**, 363 (1981).
39. C. González and H.B. Schlegel. *J. Phys. Chem* **94**, 5523 (1990).
40. L. Deng and T. Ziegler. *Int. J. Quantum Chem.* **52**, 731 (1994).
41. (a) U. Pidun, C. Boehme, and G. Frenking. *Angew. Chem. Int. Ed. Engl.* **35**, 2817 (1996); (b) O. Gonzalez-Blanco, V. Branchadell, K. Monteyne, and T. Ziegler. *Inorg. Chem.* **37**, 1744 (1998); (c) J. Li, G. Schreckenbach, and T. Ziegler. *J. Am. Chem. Soc.* **117**, 486 (1995); (d) E. Folga and T. Ziegler. *J. Am. Chem. Soc.* **115**, 5150 (1993).
42. R. Poli. *Chem. Rev.* **96**, 2135 (1996).
43. (a) S. Kristyán and P. Pulay. *Chem. Phys. Lett.* **229**, 175 (1994); (b) T.C. Wright. *J. Chem. Phys.* **105**, 7579 (1996); (c) J.M. Pérez-Jordà and A.D. Becke. *Chem. Phys. Lett.* **233**, 134 (1995); (d) E. Ruiz, D.R. Salahub, and A. Vela. *J. Phys. Chem.* **100**, 12 265 (1996); (e) A. García, E.M. Cruz, C. Sarasola, and J.M. Ugalde. *J. Phys. Chem. A*, **101**, 3021 (1997).
44. (a) E. Vedejs and K.A.J. Snoble. *J. Am. Chem. Soc* **95**, 5778 (1973); (b) M. Nagayama, O. Okumura, S. Noda, and A. Mori. *J. Chem. Soc. Chem. Commun.* 841 (1973).
45. M. Torrent, L. Deng, M. Duran, M. Solà, and T. Ziegler. *Organometallics*, **16**, 13 (1997);
46. M. Torrent, L. Deng, and T. Ziegler. *Inorg. Chem.* **37**, 1307 (1998).
47. S. Dapprich, G. Ujaque, F. Maseras, A. Lledós, D.G. Musaev, and K. Morokuma. *J. Am. Chem. Soc.* **118**, 11 660 (1996).
48. A.J. DelMonte, J. Haller, K.N. Houk, K.B. Sharpless, D.A. Singleton, T. Strassner, and A.A. Thomas. *J. Am. Chem. Soc* **119**, 9907 (1997).
49. A. Rosa, A.W. Ehlers, E.J. Baerends, J.G. Snijders, and G. te Velde. *J. Phys. Chem.* **100**, 5690 (1996).
50. (a) K.P. Gable and T.N. Phan. *J. Am. Chem. Soc.* **115**, 3036 (1993); (b) *J. Am. Chem. Soc.* **116**, 833 (1994).
51. M.A. Pietsch, T.V. Russo, R.B. Murphy, R.L. Martin, and A.K. Rappé. *Organometallics*, **17**, 2716 (1998).
52. (a) T. Ziegler, J.G. Snijders, and E.J. Baerends. *J. Chem. Phys.* **74**, 1271 (1981); (b) G. Schreckenbach, J. Li, and T. Ziegler. *Int. J. Quantum Chem.* **56**, 477 (1995).
53. C. Limberg and R. Köppe. *Inorg. Chem.* **38**, 2106 (1999).